Journal of Achievements in Materials and Manufacturing Engineering
VOLUME 48 ISSUE 2 October 2011

Structure and physical properties of Fe-based metallic glasses with Ni and Co addition

S. Lesz*, R. Nowosielski
Institute of Engineering Materials and Biomaterials, Silesian University of Technology, ul. Konarskiego 18a, 44-100 Gliwice, Poland
* Corresponding author: E-mail address: sabina.lesz@polsl.pl

Received 07.08.2011; published in revised form 01.10.2011

Materials

ABSTRACT

Purpose: The main aim of the paper was investigation of structure and physical properties of Fe-based metallic glasses with Ni and Co addition.

Design/methodology/approach: The structure was characterized by X-ray diffraction (XRD) method, transmission electron microscope (TEM), scanning electron microscope (SEM). The measurement of physical properties (magnetic and mechanical) were made. The magnetic properties contained initial magnetic permeability μ_i, coercive force H_c and magnetic after-effects $\Delta\mu/\mu$ measurements were determined by the Maxwell-Wien bridge, coercivemeter and with the use of automatic device for measurements magnetic permeability, respectively. Microhardness tests were performed on Vickers microhardness tester.

Findings: The XRD and TEM investigations revealed that the studied ribbons were amorphous. The SEM images showed that studied fractures morphology of ribbons is changing from smooth fracture inside with narrow dense veins pattern on surface having contact with the copper roller during casting to fine (shell) chevron pattern on surface freely solidified. The changing of chosen soft magnetic and mechanical properties obtained for samples with different thickness is a result of the non-homogenous amorphous structure of tested metallic glasses.

Practical implications: The successful preparation of the Fe-based metallic glasses with Ni and Co addition from industrial raw materials will benefit cost-effective development of functional ferromagnetic materials and may be utilized in construction of magnetic cores such as common mode choke coils and noise filters.

Originality/value: In this work, an attempt has been made to prepare the Fe-based metallic glasses more economically by means of replacement of high purity materials with industrial materials (ferroalloys).

Keywords: Amorphous materials; Industrial materials; XRD, SEM and TEM method; Magnetic properties; Microhardness

Reference to this paper should be given in the following way:
S. Lesz, R. Nowosielski, Structure and physical properties of Fe-based metallic glasses with Ni and Co addition, Journal of Achievements in Materials and Manufacturing Engineering 48/2 (2011) 145-152.

1. Introduction

Since the first Fe-based metallic glasses was synthesized by rapid solidification technique in 1967, a great number of amorphous alloys have been produced for the last decades [1-18]. It is well known that Fe, Co- Ni-based metallic glasses found before 1990 are the most attractive due to many superior properties such as high mechanical strength, good deformability in the supercooled liquid region, strong corrosion resistance, low hysteresis losses and low current losses under cyclic magnetic excitation, as well as abundant natural resources and relatively low material cost [1-22].

Fe, Co- Ni-based metallic glasses due to the low glass-forming ability (GFA) require high cooling rates above 10^5 K·s^{-1} for glass formation and the resulting sample thickness is limited to less than about 0.05 mm [1]. Recently, new multicomponent alloy system with much lower critical cooling rates in the Mg-, Ln-, Zr, Fe-, Pd-Cu-, Pd-Fe-, Ti- and Ni-based alloy systems were prepared. Figure 1 shows the relationship between the critical cooling rate (R_c), maximum sample thickness (t_{max}) and reduced glass transition temperature (T_g/T_m) for amorphous alloys [1]. The lowest R_c is as low as 0.10 K·s^{-1} for the Pd-Cu-Ni-P alloy and the t_{max} reaches values as large as about 100 mm. Alloys with low R_c and t_{max} over 1 mm are known as bulk metallic glasses (BMG). The recent improvement of the glass-forming ability (GFA) reaches 6-7 orders for the critical cooling rate and 3-4 orders for the maximum thickness. With increasing (T_g/T_m) the GFA increases, too.

The development of Fe-based ferromagnetic BMG with high GFA has become a very hot research topic because of the soft magnetic properties and high fracture strength (σ_f). At present, many researches have been performed for the $[(Fe_{1-x-y}Co_xNi_y)_{0.75}B_{0.2}Si_{0.05}]_{96}Nb_4$ glassy alloy system preparation from high purity materials, which exhibits high GFA, good soft magnetic properties and high fracture strength.

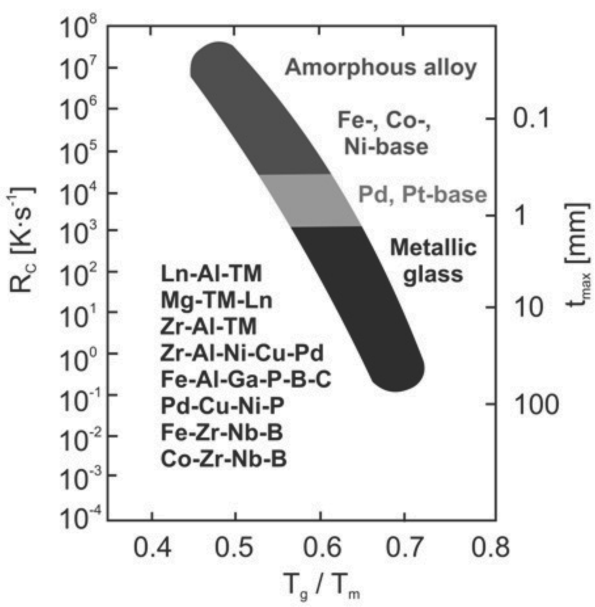

Fig. 1. Relationship between the critical cooling rate (R_c), maximum sample thickness for glass formation (t_{max}) and reduced glass transition temperature (T_g/T_m) for bulk amorphous alloys [1]

Figures 2 and 3 show the compositional dependence of thermal stability associated with glass transition temperature (T_g) and supercooled liquid region (ΔT_x), defined by the difference between (T_g) and crystallization temperature (T_x) of the $[(Fe_{1-x-y}Co_xNi_y)_{0.75}B_{0.2}Si_{0.05}]_{96}Nb_4$ glassy alloys, respectively [2,4]. The T_g shows a significant change with Ni content and decreases almost linearly from 810 to 760 K with increasing Ni content. There is no distinct change in T_g with the Co to Fe concentration ratio (Fig. 2) [4].

Figure 4 shows the compositional dependence of compressive fracture strength (σ_f) for $[(Fe_{1-x-y}Co_xNi_y)_{0.75}B_{0.2}Si_{0.05}]_{96}Nb_4$ glassy alloys in rods form [4]. The high yield strength of over 4000 MPa is obtained in the composition range of 0-1.0 Co and 0-0.7 Ni. Further increase in Ni content causes the decrease in strength to about 3700 MPa.

The (ΔT_x) shows a maximum value of about 70 K in the range of 0.50-0.65 Fe, 0.35-0.45 Co and 0-0.15 Ni and keeps high values of over 60 K in the Ni content range up to 0.35 Ni (Fig. 3) [2].

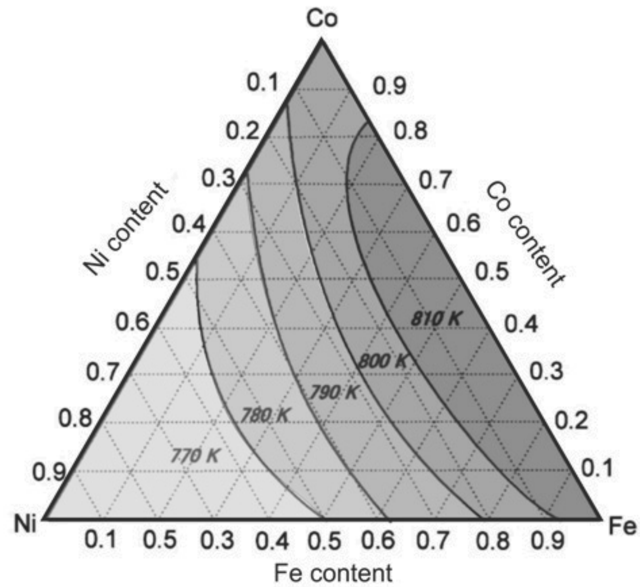

Fig. 2. Compositional dependence of glass transition temperature (T_g) for $[(Fe_{1-x-y}Co_xNi_y)_{0.75}B_{0.2}Si_{0.05}]_{96}Nb_4$ glassy alloys [4]

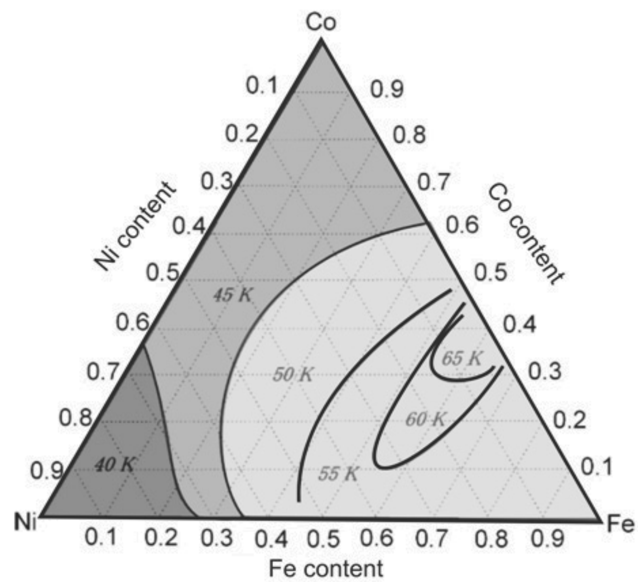

Fig. 3. Compositional dependence of supercooled liquid region (ΔT_x) for $[(Fe_{1-x-y}Co_xNi_y)_{0.75}B_{0.2}Si_{0.05}]_{96}Nb_4$ glassy alloys [2]

Compositional dependence of the diameter for glass formation by copper mold casting for $[(Fe_{1-x-y}Co_xNi_y)_{0.75}B_{0.2}Si_{0.05}]_{96}Nb_4$ glassy alloys is shown in Fig. 5 [2].

It has been reported by Inoue that $(Fe_{0.75}B_{0.15}Si_{0.1})_{96}Nb_4$ bulk glassy alloy exhibits large GFA [13]. Co and Ni elements were added into the in this alloy system supports the Inoue's rules for stabilization of supercooled metallic liquid, i.e.: multi component, significant atomic size mismatches and negative heat of mixing, as the mixing enthalpies of the atomic pairs, i.e. Co-Si (-21 kJ·mol^{-1}), Co-Nb (-25 kJ·mol^{-1}), Ni-Si (-23 kJ·mol^{-1}) and Ni-B(-9 kJ·mol^{-1}), are negative and their absolute values are large. The sequence of atomic size in these compounded alloy goes as follows: Nb > Ni > Co > Fe > Si > B [2-5].

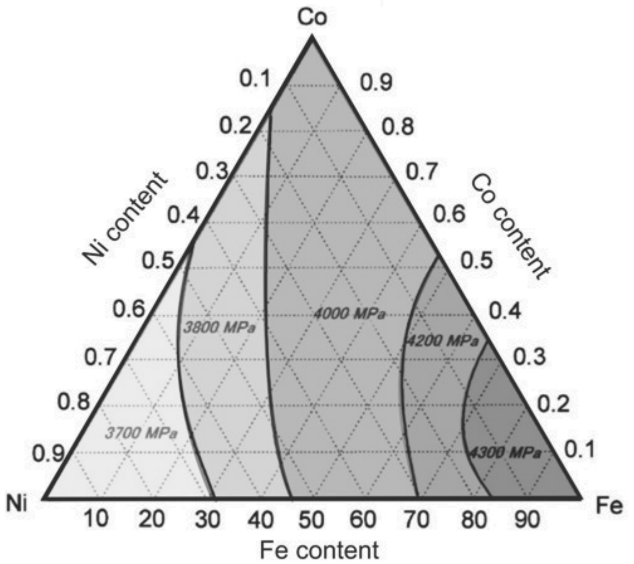

Fig. 4. Compositional dependence of compressive fracture strength (σ_f) for $[(Fe_{1-x-y}Co_xNi_y)_{0.75}B_{0.2}Si_{0.05}]_{96}Nb_4$ glassy alloys [4]

Table 1 summarizes maximum diameter (ϕ_{max}), thermal stability: (T_g), (ΔT_x), (T_g/T_m), magnetic properties: Curie temperature (T_C), saturation magnetization (I_s), coercive force (H_c), permeability (μ_e) and mechanical properties: Vickers hardness (H_v) Young's modulus (E), compressive fracture strength (σ_f), compressive true elastic strain ($\varepsilon_{c,p}$) of the cast $(Fe_{0.75}B_{0.15}Si_{0.1}]_{96}Nb_4$, $[(Fe_{0.8}Co_{0.1}Ni_{0.1})_{0.75}B_{0.2}Si_{0.05}]_{96}Nb_4$.$[(Fe_{0.6}Co_{0.1}Ni_{0.3})_{0.75}B_{0.2}Si_{0.05}]_{96}Nb_4$, $[(Fe_{0.6}Co_{0.2}Ni_{0.2})_{0.75}B_{0.2}Si_{0.05}]_{96}Nb_4$, $[(Fe_{0.6}Co_{0.3}Ni_{0.1})_{0.75}B_{0.2}Si_{0.05}]_{96}Nb_4$ glassy alloys prepared from high purity materials [3]. Many metallic glasses have been fabricated from high purity raw materials. The high purity of raw materials and the strict processing cause a high cost for production of metallic glasses, which is one of the key problems restricting their the wide industrial applications. Thus, the search for Fe-base metallicglasses prepared from low cost industrial raw materials is important for practical application [23-25].

Some industrial ferroalloys having high carbon and high silicon contents exhibited high glass forming ability (GFA) [24]. On the other hand the presence of even traces of oxygen and other impurities would induce the heterogeneous nucleation and cause difficulties for fully amorphous structure and pose a problem with obtaining eutectic composition [23, 25]. Therefore the solution of these limitations is part of interesting and innovative research work. This paper presents results of investigation of structure and physical properties of Fe-based metallic glasses with Ni and Co addition prepared from industrial raw materials.

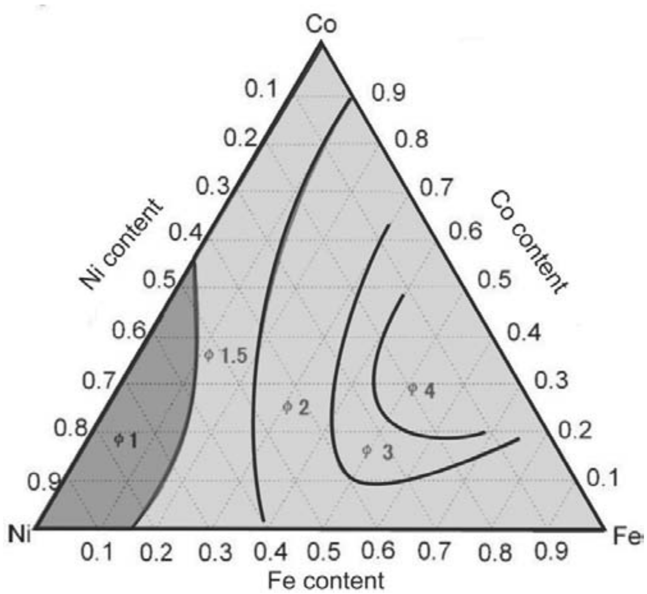

Fig. 5. Compositional dependence of the diameter (ϕ_{max}) for glass formation by copper mold casting for $[(Fe_{1-x-y}Co_xNi_y)_{0.75}B_{0.2}Si_{0.05}]_{96}Nb_4$ glassy alloys [2]

2. Materials and research methodology

The aim of this paper is analysis of the structure and physical properties of $[(Fe_{0.6}Co_{0.2}Ni_{0.2})_{0.75}B_{0.2}Si_{0.05}]_{96}Nb_4$ alloy. The Fe-based master alloy ingots with compositions of $Fe_{43}Co_{14.5}Ni_{14.5}B_{19}Si_5Nb_4$ were prepared by melting the mixtures of pure Fe, Co metals and ferroalloys: Fe-B , Fe-Nb, Fe-Si, which contains Fe and 14.5 mass% of B, 68.5 mass% of Nb, 57.2 mass% of Si, respectively and other constituents, such as aluminium, carbon, sulfur, phosphorus and their oxides in remainder. The master alloy was melted in a quartz crucible using an induction coil. Ribbons with thickness of 0.07 and 0.25 mm and width of 2.3 mm were manufactured by the "chill-block melt spinning" (CBMS) technique, which is a method of continuous casting of the liquid alloy on the surface of a turning copper based roller [6,10,15]. The casting conditions include linear speed of copper roller: 20 m/s and ejection over-pressure of molten alloy: 0.02 MPa.

The microstructure of the ribbons was examined by X-ray diffraction (XRD), TEM and SEM method.

The X-ray method has been performed by the use of diffractometer X-Pert PRO MP with filtered Co-Kα radiation. The data of diffraction lines were recorded by "step-scanning" method in 2θ range from 40° to 100°.

Table 1.
Maximum diameter (ϕ_{max}), thermal stability: (T_g), (ΔT_x), (T_g/T_m), magnetic properties: Curie temperature (T_C), saturation magnetization (I_s), coercive force (H_c), permeability (μ_e) and mechanical properties: Vickers hardness (H_v) Young's modulus (E), compressive fracture strength (σ_f), compressive true elastic strain ($\varepsilon_{c,p}$) of the cast $(Fe_{0.75}B_{0.15}Si_{0.1})_{96}Nb_4$ (I), $[(Fe_{0.8}Co_{0.1}Ni_{0.1})_{0.75}B_{0.2}Si_{0.05}]_{96}Nb_4$ (II). $[(Fe_{0.6}Co_{0.1}Ni_{0.3})_{0.75}B_{0.2}Si_{0.05}]_{96}Nb_4$ (III), $[(Fe_{0.6}Co_{0.2}Ni_{0.2})_{0.75}B_{0.2}Si_{0.05}]_{96}Nb_4$ (IV), $[(Fe_{0.6}Co_{0.3}Ni_{0.1})_{0.75}B_{0.2}Si_{0.05}]_{96}Nb_4$ (V) glassy alloys prepared from high purity materials [3]

Alloy	Diameter	Thermal stability			Magnetic properties				Mechanical properties			
	ϕ_{max}	T_g	ΔT_x	T_g/T_m	T_C	I_s	H_c	μ_e	H_v	E	σ_f	$\varepsilon_{c,p}$
	mm	K	K		K	T	A·m^{-1}			GPa	MPa	
I	1.5	832	45	0.611	593	1.20	3.7	9600	1060	175	3250	0.001
II	2.5	818	55	0.606	613	1.10	3.0	16000	1230	208	4225	0.005
III	3.0	792	60	0.608	554	0.80	2.5	19000	1170	205	4070	0.004
IV	4.0	800	65	0.611	598	0.86	2.5	19000	1210	210	4160	0.002
V	4.0	813	65	0.613	643	0.90	2.0	21000	1240	210	4200	0.002

In order to conduct structural study, the electron microscope TESLA BS 540 in magnification of 100000× was used. Thin foils for TEM observation (from central part of tested samples) were prepared by an electrolytic polishing method after previous mechanical grinding.

The morphology of fracture surfaces after decohesion was observed in scanning electron microscope ZEISS SUPRA 25.

Magnetic measurements of ribbons (determined at room temperature) included following properties:

(1) relative magnetic permeability μ_i - determined by Maxwell-Wien bridge at a frequency of 1030 Hz and magnetic field H=0.5 A/m;
(2) coercive field - measured by coercivemeter;
(3) intensity of magnetic after effect $\Delta\mu/\mu$ also defined as magnetic permeability relaxation, where μ is the initial magnetic permeability measured at time t_1=30 s and t_2=1800 s after demagnetization. The investigations were performed with the use of automatic device for measurements magnetic permeability [12].

Microhardness was measured with a use of the Vickers hardness tester FUTURE-TECH FM-700 under a load of 49 N (50G) [26]. The microhardness was measured on the shining surface of ribbons according to pattern presented in Fig. 6.

3. Results and discussion

It was found from the obtained results of structural studies performed by X-ray diffraction (XRD), transmission electron microscopy (TEM), that in as quenched state the structure of the ribbons with thickness of both 0.07 mm and 0.25 mm of $Fe_{43}Co_{14.5}Ni_{14.5}B_{19}Si_5Nb_4$ alloy consists of amorphous phase (Figs. 7, 8, 9). The X-ray tests prove that the structure of the both of ribbons of $Fe_{43}Co_{14.5}Ni_{14.5}B_{19}Si_5Nb_4$ alloy is amorphous, which is seen on the diffraction pattern in the form of a broad-angle peak originating from amorphous phase (Fig. 7). Obtained results of structural studies performed by XRD are corresponding with the TEM micrograph (Figs. 8, 9). The TEM images revealed only some changes in contrast, which is characteristic for amorphous structure. The electron diffraction patterns consisted only of the halo rings. Broad diffraction halo can be seen for both of tested ribbons, indicating the formation of a glassy phase.

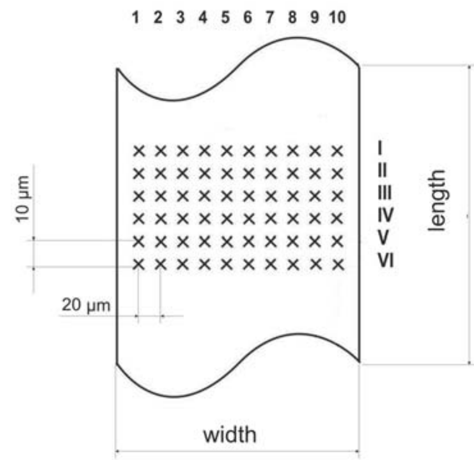

Fig. 6. The pattern of microhardness measurements

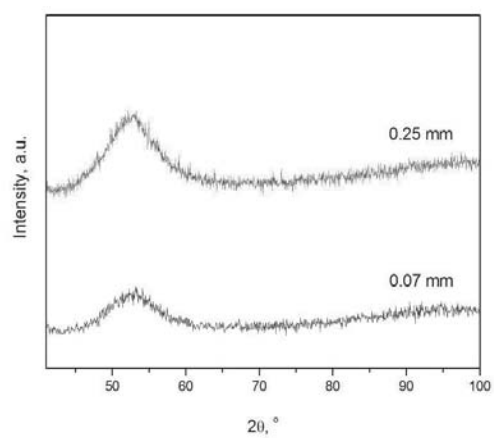

Fig. 7. X-ray diffraction pattern of $Fe_{43}Co_{14.5}Ni_{14.5}B_{19}Si_5Nb_4$ ribbons with thickness of 0.07 mm and 0.25 mm

The analysis of data of magnetic properties i.e. μ_i and H_c allow to classify the alloy as a soft magnetic material (Table 2). The ribbons with thickness of 0.07 mm have better magnetic properties (H_c=6.0 A/m, μ_i=1800, $\Delta\mu/\mu$=11.0, Table 2) than ribbons with thickness of 0.25 mm (H_c=10.0 A/m, μ_i=1000, $\Delta\mu/\mu$=4.5, Table 2) of alloy.

Table 2.
Magnetic properties (H_c – coercivity, μ_i – initial magnetic permeability, $\Delta\mu/\mu$ – magnetic after effects) of $Fe_{43}Co_{14.5}Ni_{14.5}B_{19}Si_5Nb_4$ ribbons with thickness of 0.07 mm and 0.25 mm

Thickness of Ribbons, mm	Magnetic properties		
	H_c, A/m	μ_i	Δμ/μ, %
0.07	6.0	1800	11.0
0.25	10.0	1000	4.5

The thinner ribbons have better magnetic properties, what suggests that the casting conditions have influence on microvoids content and thereby on magnetic properties.

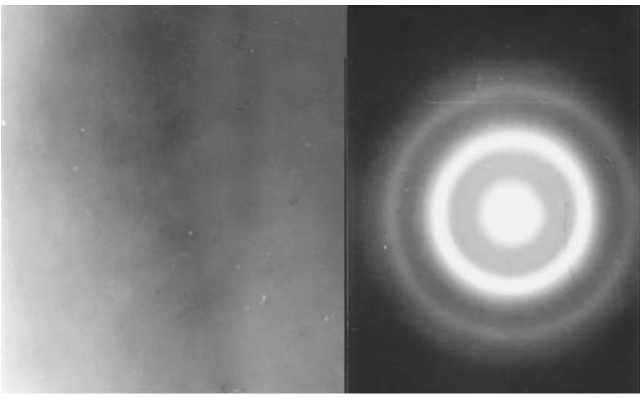

Fig. 8. TEM micrograph of $Fe_{43}Co_{14.5}Ni_{14.5}B_{19}Si_5Nb_4$ ribbons with thickness of 0.07 mm. Mag=100000×

These excellent magnetic properties (Table 2) lead us to expect that the Fe-based amorphous alloy could be used as a new engineering and functional material intended for parts of inductive components. The microvoids content is often examined using magnetic after effects ($\Delta\mu/\mu$) measurements. The value of $\Delta\mu/\mu$ increases with increasing of microvoids into materials [12].

The obtained values of H_c of the ribbons with thickness of 0.07 mm of $Fe_{43}Co_{14.5}Ni_{14.5}B_{19}Si_5Nb_4$ alloy are similar than in other alloys with the similar chemical composition investigated by Shen whose results for $[(Fe_{0.6}Co_{0.2}Ni_{0.2})_{0.75}B_{0.2}Si_{0.05}]_{96}Nb_4$ alloys: H_c=2.5 A/m [3].

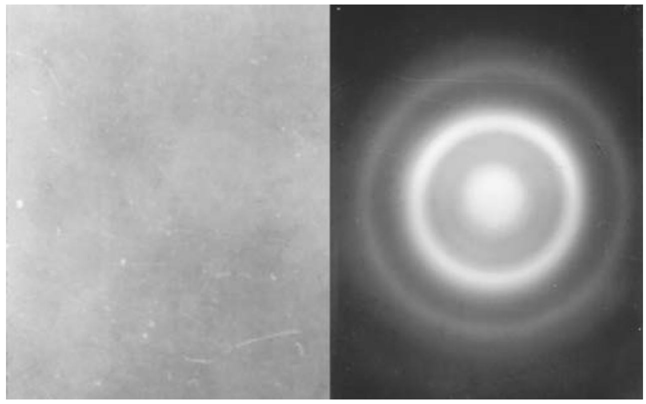

Fig. 9. TEM micrograph of $Fe_{43}Co_{14.5}Ni_{14.5}B_{19}Si_5Nb_4$ ribbons with thickness of 0.25 mm. Mag=100000×

Results of microhardness experiments of $Fe_{43}Co_{14.5}Ni_{14.5}B_{19}Si_5Nb_4$ ribbons with thickness of 0.07 mm and 0.25 mm are presented in Table 3 and 4, respectively.

The results of microhardness measurements points to changeable microhardness of $Fe_{43}Co_{14.5}Ni_{14.5}B_{19}Si_5Nb_4$ ribbons with thickness of 0.07 mm and 0.25 mm depended on place of measurements. Microhardness H_v varies between 1055-1404 MPa on the margin of ribbons and 988-1404 MPa in centre of $Fe_{43}Co_{14.5}Ni_{14.5}B_{19}Si_5Nb_4$ ribbons with thickness of 0.07 mm (Table 3). Similarly microhardness H_v varies between 1055-1519 MPa on the margin of ribbons and 927-1302 MPa in centre of ribbons with thickness of 0.25 mm (Table 4). These differences may suggest that process of solidification of amorphous ribbons is different in centre and on the margin and is connected with cooling rate of ribbons during casting. The results of microhardness of ribbons are in agreement with findings in [3] (1210 H_v).

The significant changes of fracture morphology of $Fe_{43}Co_{14.5}Ni_{14.5}B_{19}Si_5Nb_4$ ribbons with thickness of both 0.07 mm and 0.25 mm after decohesion are corresponding to the observed microhardness changes.

Morphology is changing from smooth fracture inside with narrow dense veins pattern in surface having contact with the copper roller during casting to fine (shell) chevron pattern in surface freely solidified (shining surface) (Figs. 10, 11).

Table 3.
Results of microhardness experiments of $Fe_{43}Co_{14.5}Ni_{14.5}B_{19}Si_5Nb_4$ ribbons with thickness of 0.07 mm

No.	1	2	3	4	5	6	7	8	9	10
I	1055	1211	1648	1302	1404	1129	988	1302	1211	1404
II	1404	1302	1519	1129	1211	1211	988	1129	1302	1404
III	1302	1302	1211	1129	1302	1404	1211	1302	1302	1302
IV	1055	1055	1055	1404	1211	1302	1055	1404	1129	1211
V	1211	1648	1211	1648	1404	1302	1129	1211	927	1129
VI	1129	1404	1129	1404	1055	1211	1302	1129	1211	1404

Table 4.
Results of microhardness experiments of $Fe_{43}Co_{14.5}Ni_{14.5}B_{19}Si_5Nb_4$ ribbons with thickness of 0.25 mm

No.	1	2	3	4	5	6	7	8	9	10
I	1519	1404	1211	1055	1129	927	988	1129	1211	1519
II	1211	1404	1519	1129	927	1211	1211	1211	1404	1129
III	1404	1302	1302	1129	1211	1129	1211	1129	1302	1129
IV	1129	1055	1211	1302	988	1211	1302	1302	1129	1302
V	1055	1302	1302	1129	927	927	988	1129	1211	1302
VI	1302	1129	1055	927	988	988	927	1211	1055	1404

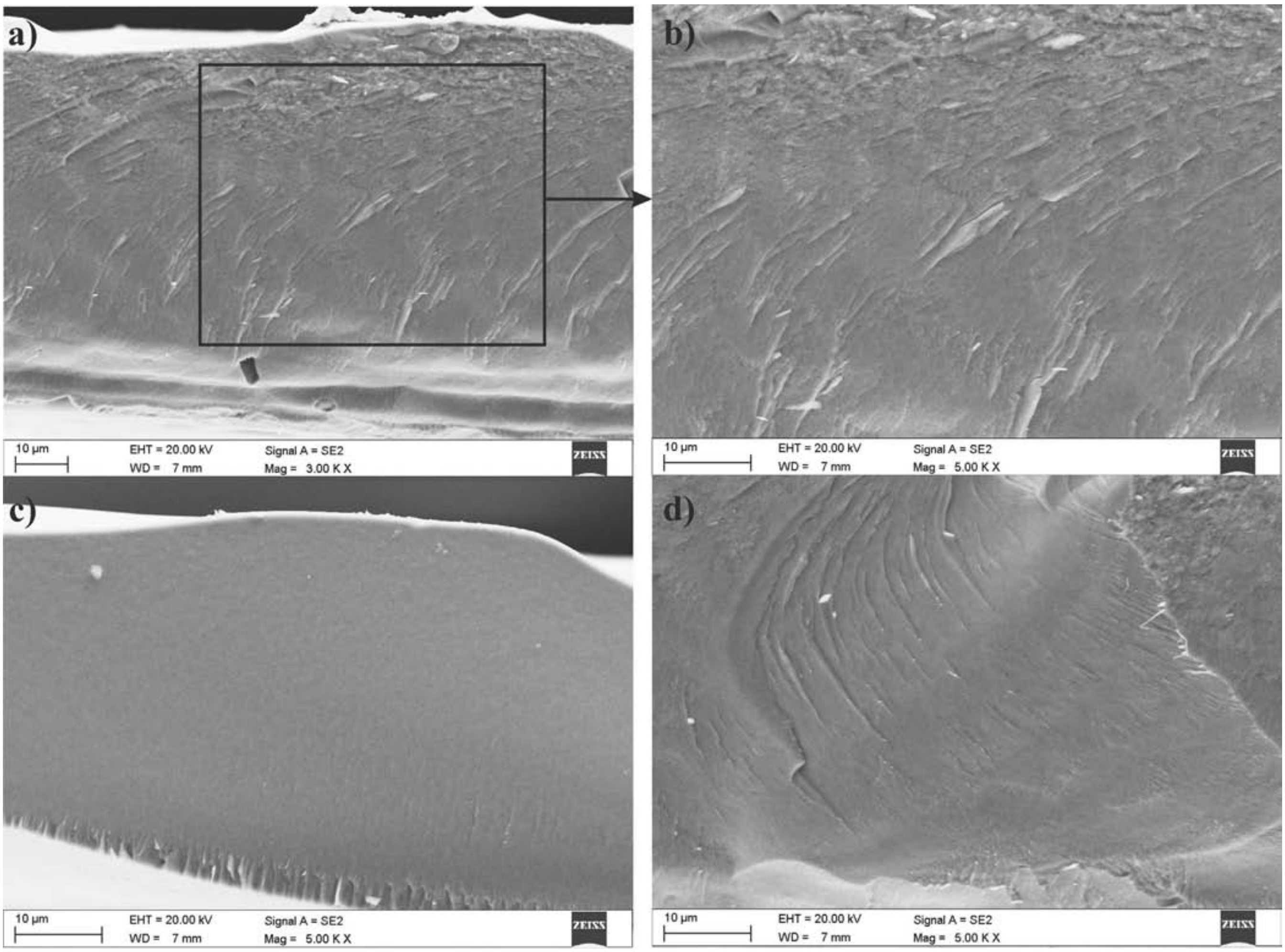

Fig. 10. SEM image of fracture surface of $Fe_{43}Co_{14.5}Ni_{14.5}B_{19}Si_5Nb_4$ ribbons with thickness of 0.07 mm after decohesion; a) and c) main view of ribbon with different morphology, b) fine (shell) chevron pattern in surface freely solidified, c) smooth fracture with narrow dense veins pattern in surface having contact with the copper roller during casting, d) central part of ribbon with different morphology (veins and shell pattern)

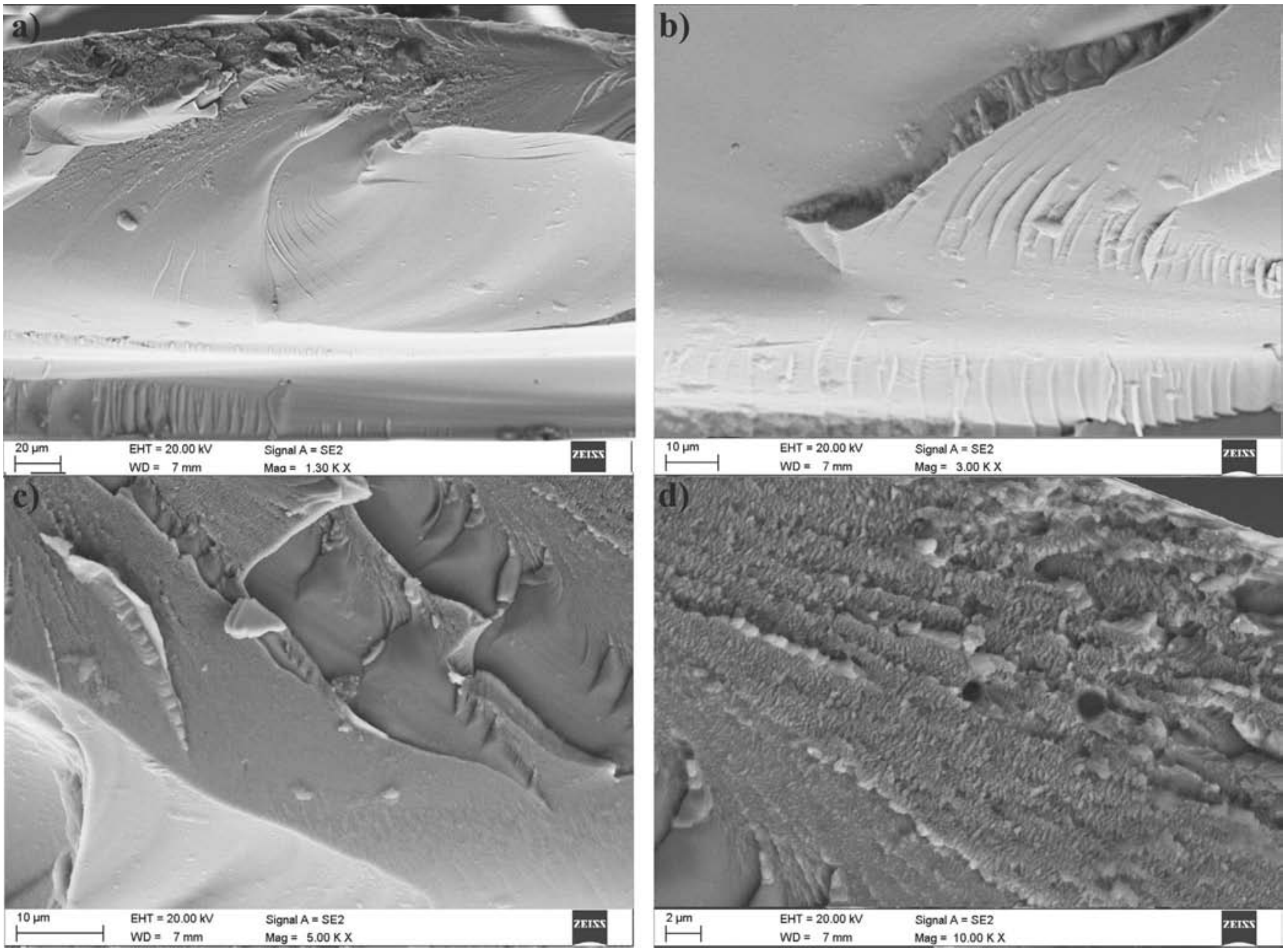

Fig. 11. SEM image of fracture surface of $Fe_{43}Co_{14.5}Ni_{14.5}B_{19}Si_5Nb_4$ ribbons with thickness of 0.25 mm after decohesion; a) main view of ribbon with different morphology, b) smooth fracture with narrow dense veins pattern in surface having contact with the copper roller during casting, c) central part of ribbon with different morphology (veins and shell pattern), d) fine (shell) chevron pattern in surface freely solidified

4. Conclusions

On the basis of the obtained results we can state that the ribbons of $Fe_{43}Co_{14.5}Ni_{14.5}B_{19}Si_5Nb_4$ alloy have amorphous structure and good soft magnetic properties. Thinner ribbons of $Fe_{43}Co_{14.5}Ni_{14.5}B_{19}Si_5Nb_4$ alloy exhibit better soft magnetic properties than the other ribbons.

The following working hypothesis was adopted: process of solidification of ribbons influences on amorphization process. The amorphous structure is different and non-homogenous on cross section and on surface of ribbons.

This hypothesis was confirmed by results of fracture morphology of $Fe_{43}Co_{14.5}Ni_{14.5}B_{19}Si_5Nb_4$ ribbons with thickness of both 0.07 mm and 0.25 mm after decohesion and with the microhardness changes on the surface of ribbons. Morphology is changing from smooth fracture inside with narrow dense veins pattern on surface having contact with the copper roller during casting to fine (shell) chevron pattern on surface freely solidified. Furthermore, investigation for example Mössbauer spectrometry has to be conducted on different thickness of ribbons in order to confirm these conclusions.

These excellent magnetic properties of the Fe-based metallic glasses with Ni and Co addition prepared from industrial raw materials will benefit cost-effective development of new engineering and functional material.

References

[1] A. Inoue, Stabilization of metallic supercooled liquid and bulk amorphous alloys, Acta Materialia 48 (2000) 279-306.

[2] Ch. Chang, B. Shen, A. Inoue, Synthesis of bulk glassy alloys in the (Fe,Co,Ni)-B-Si-Nb system, Materials Science and Engineering A 449-451 (2007) 239-242.

[3] B. Shen, Ch. Chang, A. Inoue, Formation, ductile deformation behaviour and soft-magnetic properties of (Fe,Co,Ni)-B-Si-Nb bulk glassy alloys, Intermetallics 15 (2007) 9-16.
[4] A. Inoue, B. Shen, A. Takeuchi, Fabrication, properties and applications of bulk glassy alloys in late transition metal-baed systems, Materials Science and Engineering A 441 (2006) 18-25.
[5] R. Nowosielski, R. Babilas, S. Griner, T. Czeppe, Structure, thermal and magnetic properties of $Fe_{43}Co_{14}Ni_{14}B_{20}Si_5Nb_4$ bulk metallic glass, Journal of Achievements in Materials and Manufacturing Engineering 38/2 (2010) 123-130.
[6] R. Babilas, R. Nowosielski, Iron-based bulk amorphous alloys, Archives of Materials Science and Engineering 44/1 (2010) 5-27.
[7] R. Nowosielski, R. Babilas, Preparation, structure and properties of Fe-based bulk metallic glasses, Journal of Achievements in Materials and Manufacturing Engineering 40/2 (2010) 123-130.
[8] S. Lesz, Preparation of Fe-Co-based bulk amorphous alloy from high purity and industrial raw materials, Archives of Materials Science and Engineering 48/2 (2011) 77-88.
[9] S. Lesz, S. Griner, R. Nowosielski, Influence of geometry of rapidly solidified rods on properties of Fe-Co-based alloy, Journal of Achievements in Materials and Manufacturing Engineering 41 (2010) 16-25.
[10] S. Lesz, D. Szewieczek, J. Tyrlik-Held, Correlation between fracture morphology and mechanical properties of NANOPERM alloys, Archives of Materials Science and Engineering 29/2 (2008) 73-80.
[11] S. Lesz, R. Babilas, M. Nabiałek, M. Szota, M. Dośpiał, R. Nowosielski: The characterization of structure, thermal stability and magnetic properties of Fe-Co-B-Si-Nb bulk amorphous and nanocrystalline alloys, Journal of Alloys and Compounds 509S (2011) 197-201.
[12] S. Lesz, Z. Stokłosa, R. Nowosielski, Influence of copper addition on properties of $(Fe_{36}Co_{36}B_{19}Si_5Nb_4)_{100-x}Cu_x$ metallic glasses, Archives of Materials Science and Engineering 38/1 (2009) 12-18.
[13] A. Inoue, B. Shen, Ch. Chang, Super-high strength of over 4000 MPa for Fe-based bulk glassy alloys in $[(Fe_{1-x}Co_x)_{0.75}B_{0.2}Si_{0.05}]_{96}Nb_4$ system, Acta Materialia 52 (2004) 4093-4099.
[14] L.A. Dobrzański, M. Drak, B. Ziębowicz, Materials with specific magnetic properties, Journal of Achievements in Materials and Manufacturing Engineering 17 (2006) 37-40.
[15] C. Suryanarayana, A. Inoue, Bulk metallic glasses, CRC Press Taylor & Francis Group Boca Raton, London, New York, 2011.
[16] R. Babilas, M. Kądziołka-Gaweł, R. Nowosielski, Structure studies of Fe-based metallic glasses by Mössbauer spectroscopy method, Journal of Achievements in Materials and Manufacturing Engineering 45/1 (2011) 7-12.
[17] B. Ziębowicz, L.A. Dobrzański, Application of nano-structural materials in manufacturing of soft magnetic composite materials $Fe_{73.5}Cu_1Nb_3Si_{13.5}B_9$ - PEHD type, Journal of Achievements in Materials and Manufacturing Engineering 24/2 (2007) 91-94.
[18] J. Konieczny, A. Borisjuk, M. Pashechko, L.A. Dobrzański, Magnetic properties of Co-based amorphous ribbon under cyclic heating and cooling, Journal of Achievements in Materials and Manufacturing Engineering 42 (2010) 42-49.
[19] R. Nowosielski, R. Babilas, S. Griner, Z. Stokłosa, Structure and soft magnetic properties of $Fe_{72}B_{20}Si_4Nb_4$ bulk metallic glasses, Archives of Materials Science and Engineering 35/1 (2009) 13-20.
[20] W. Pilarczyk, R. Nowosielski, R. Babilas, An attempt of selected metallic glasses producing with Fe and Ni matrix, Archives of Materials Science and Engineering 41/1 (2010) 5-12.
[21] L.A. Dobrzański, M. Drak, Hard magnetic composite materials Nd-Fe-B with additions of iron and X2CrNiMo-17-12-2 steel, Journal of Alloys and Compounds 449/1-2 (2008) 88-92.
[22] B. Ziębowicz, D. Szewieczek, L.A. Dobrzański, New possibilities of application of composite materials with soft magnetic properties, Journal of Achievements in Materials and Manufacturing Engineering 20 (2007) 207-210.
[23] Z.H. Gan, H.Y. Yi, J. Pu, J.F. Wang, J.Z. Xiao, Preparation of bulk amorphous Fe-Ni-P-B-Ga alloys from industrial raw materials, Scripta Materialia 48 (2003) 1543-1547.
[24] H. Li, S. Yi, Fabrication of bulk metallic glasses in the alloy system Fe-C-Si-B-P-Cr-Mo-Al using hot metal and industrial ferro-alloys, Materials Science and Engineering A 449-451 (2007) 189-192.
[25] Y. Hu, M.X. Pan, L. Liu, Y.H. Zhao, D.Q. Zhao, W.H. Wang, Synthesis of Fe-based bulk metallic glasses with low purity materials by multi-metalloids addition, Materials Letters 57 (2003) 2698-2701.
[26] PN-EN ISO 6507 - 1:2007. Metallic materials - Vickers hardness test - Part 1: Test method.